Proceedings of the 18th International Symposium on the Packaging and Transportation of Radioactive Materials
PATRAM 2016
18-23 September 2016, Kobe, Japan

Paper No. 6006

Acceleration measurement campaign on CEA type-B packages

Claude LEROY
CEA Cadarache, France

Nicolas BAUMET
CEA Cadarache, France

Adrien PESENTI
DEMA, Seyssinet, France

Abstract

The mechanical studies for type-A and type-B packages are focused in part on the tie-down system (in application of Art. 607, 613 and 638 of IAEA SSR-6 2012 edition). More specifically, stresses in the attachment points and tie-down members are analysed with respect to either the maximum inertial forces (routine conditions of transport (RCT) or normal conditions of transport (NCT)), or the cyclic loads (RCT).

Appendix IV of IAEA Advisory Material No. SSG-26 indicates the package acceleration factors to be considered when checking the attachment points. These maximal values are not given for the purpose of a fatigue analysis. Other sources of acceleration input are available from the public or private field (e.g. NF EN 12195 standard, 1989 PATRAM paper by AREVA TN on NTL flasks, 2013 PATRAM poster by the CEA on CADM casks, etc.). These values are currently the subject of an IAEA international working group.

In this context and further to some questions on fatigue, the French Alternative Energies and Atomic Energy Commission (CEA) is implementing a new acceleration measurement campaign on some of its own type-B packages. This is the case for the LR144 design which is a 20-tonne upright cylindrical-shaped package with four anchor points on the upside with a specific frame.

The acceleration components are being monitored over time. The maximum accelerations and the number of cycles are calculated afterwards, which allows us to use several signal processing methods. This paper describes the methodology chosen for this campaign: the measuring system (sensors, signal conditioning, recording), the set-up, and the analysis. It also discusses the most relevant results for different road conditions and specific events.

Introduction

The CEA and its subcontractor DEMA conducted acceleration measurements on the LR144 transport packing during a road trip without its radioactive contents.

The LR144 is a type-B transport package that is vertical, cylindrical in shape, weighs 20 tonnes, and can be anchored by four points located at the top part of the package to a specific transport trailer.

These tests involved:

- Continuously measuring the acceleration of the transport package and its trailer in three directions (longitudinal, transverse and vertical)

- Defining the signal processing methods making it possible to determine the acceleration peaks and the number of acceleration cycles in all three directions so these values can be used in

fatigue design calculations for anchor parts.
The test conditions were those of a routine transport operation.

Accelerometer positions

The data acquisition system was installed on the trailer.
Two accelerometers were positioned on the LR144 transport package close to the anchor screws. Two other accelerometers were positioned at the base of the frame vertically to the side rails on the trailer. The objective was to measure the trailer's accelerations.

Figure 1: General view of the trailer

The accelerometers were all oriented according to the same coordinates:

- longitudinal x axis (positive end to the front)
- transverse y axis (positive end to the left)
- vertical z axis (positive end to the top).

LR144 accelerometers

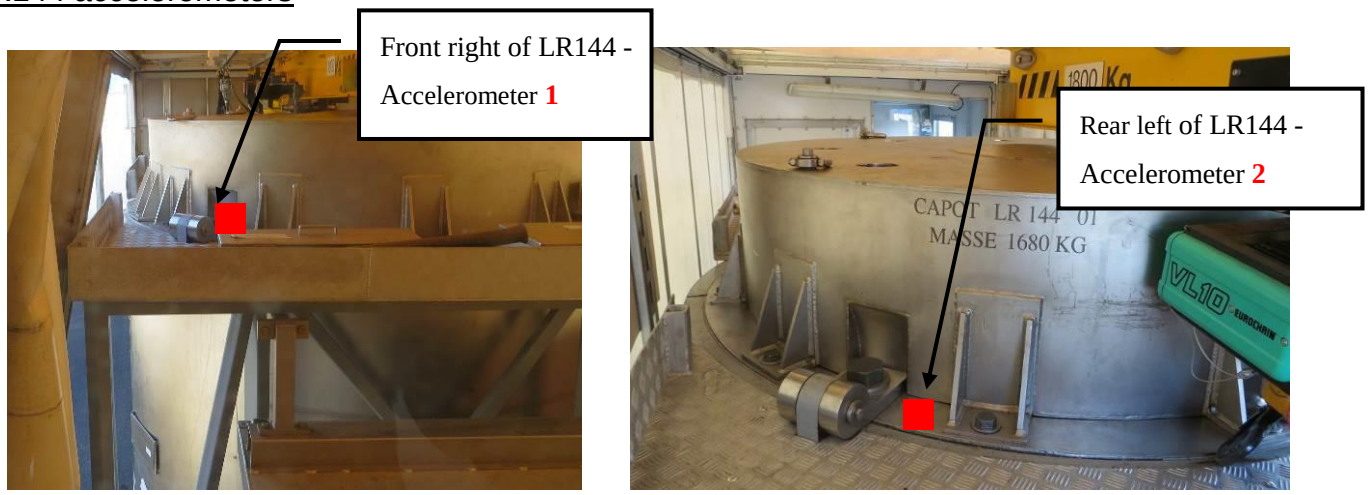

Figure 2: Location of the two accelerometers on the transport package

The two accelerometers were positioned diametrically opposite each other on the transport package and placed on the upper side of the LR144 as close as possible to the anchor screws.

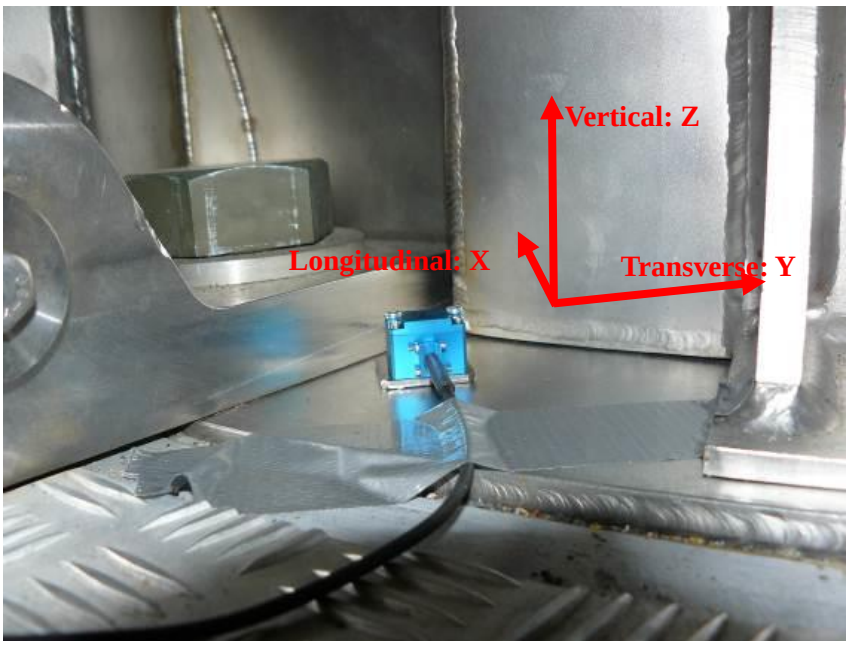

Figure 3: View of accelerometer No. 2 on the upper side of LR144

Trailer accelerometers

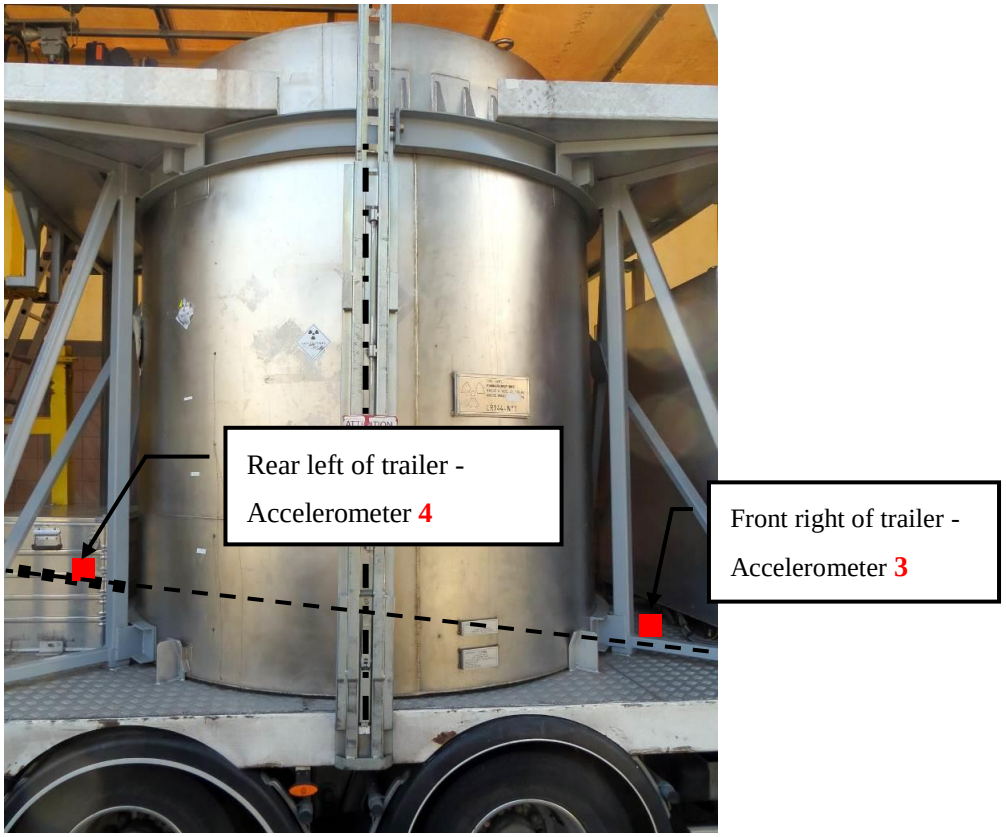

Figure 4: Location of the accelerometers on the trailer

The two accelerometers were positioned on diametrically opposite sides of the trailer, on the horizontal sections of the frame above the side rails of the trailer.

Figure 5: View of accelerometer 4 in position on the frame

Trip

The acceleration measurements were performed during the transportation of the LR144 package from the CEA Marcoule Centre to the town of Dessel in Belgium.

Measurements were recorded during the first day of transport, from the CEA Marcoule Centre to nearby the town of Macon. Measurements were recorded for 270 min, i.e. 4 h and 25 min.

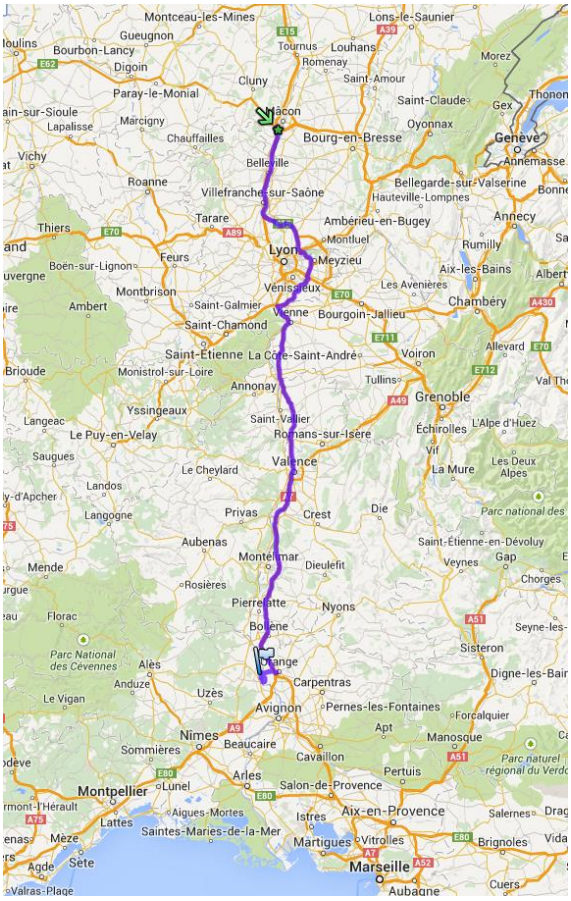

Figure 6: View of the entire trip

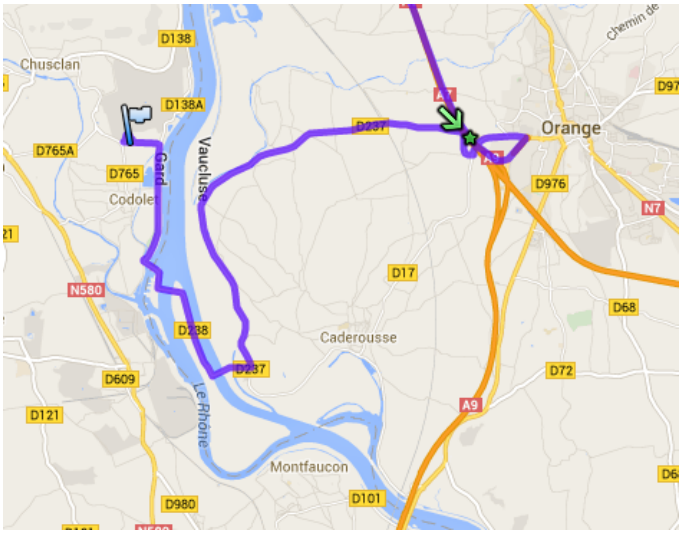

Figure 7: Detail of the trip on the national road

The recorded trip covered a distance of 282 km on the motorway and 18 km on the national road. All significant events (bends, breaking, etc.) were recorded.

Post-processing the recordings

Measurements were recorded for a duration of 4 h and 25 min. With a sampling frequency of 1000 Hz and 12 signals (4 sensors x 3 directions), the total number of samples was 191,106. The size of the resulting ASCII file - 2 Go - required using specific software designed to process large volumes of data. We used the NI DIADEM software.

Processing was performed in three stages:

1. The file was first split into two parts: one part covering the trip on the national road, and the other part on the motorway.

2. A filter was then applied to eliminate background noise: a Butterworth low-pass filter from 4 to 20 Hz.

3. Last of all, a counting algorithm was applied to the signal: RainFlow or PATRAM.

Load cycle counting method

Two counting methods are described below:

- The PATRAM method is identical to the method used to classify the acceleration levels described at the PATRAM conference in 1989 (see reference [1]). This method consists in retaining the maximum value reached for each time frame where the signal retains the same sign.

- The RainFlow method counts the load cycles and thus provides information on the variations rather than the deceleration levels.

These two counting methods are illustrated below.

Signal to process

The signal to process is first discretised according to classes (-6 to 6 in this case).

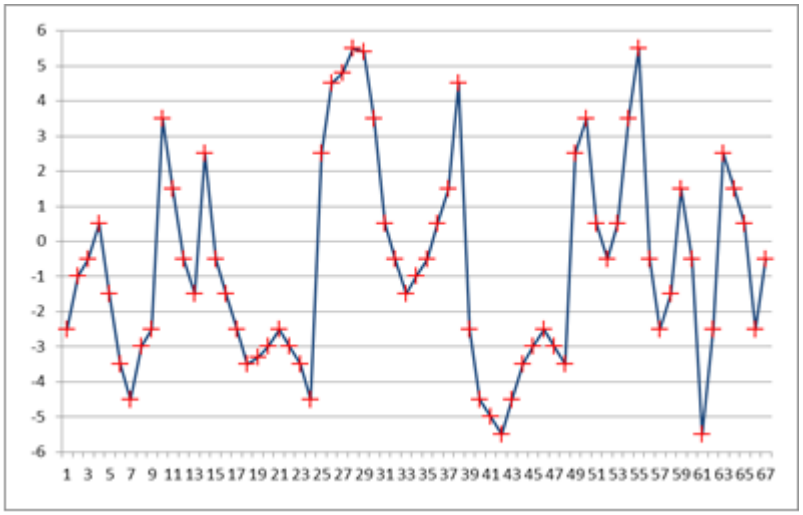

Figure 8: Example of a signal to process

The signal is composed of 67 samples classified into 12 classes from -6 to 6.

Extracting extrema

The two processing methods require first extracting the extrema. The basic signal therefore becomes:

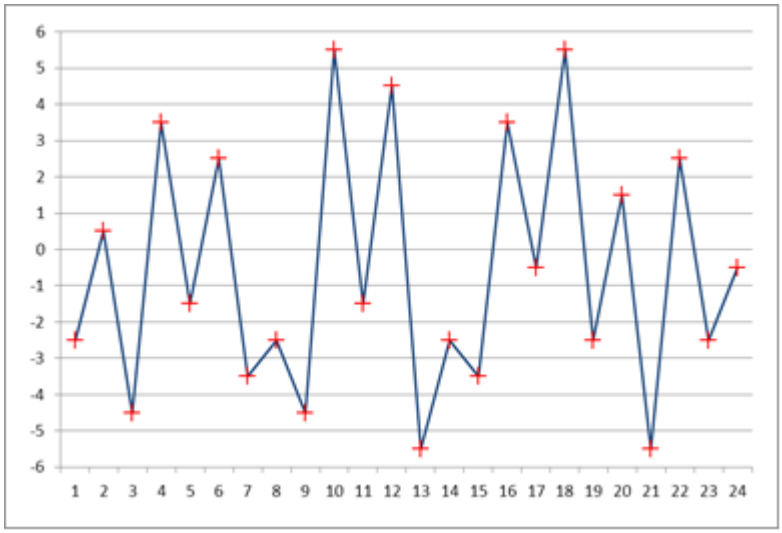

Figure 9: Processed signal after extracting the extrema

In numerical form, this is: -3,1,-5,4,-2,3,-4,-3,-5,6,-2,5,-6,-3,-4,4,-1,6,-3,1,-6,3,-3,-1.

Counting

PATRAM method

The PATRAM method consists in retaining the maximum reached for each time frame where the signal retains the same sign (the time frames are bounded by the green dotted vertical lines). To eliminate noise-related effects on the signals, the first class is not taken into account (hatched zone).

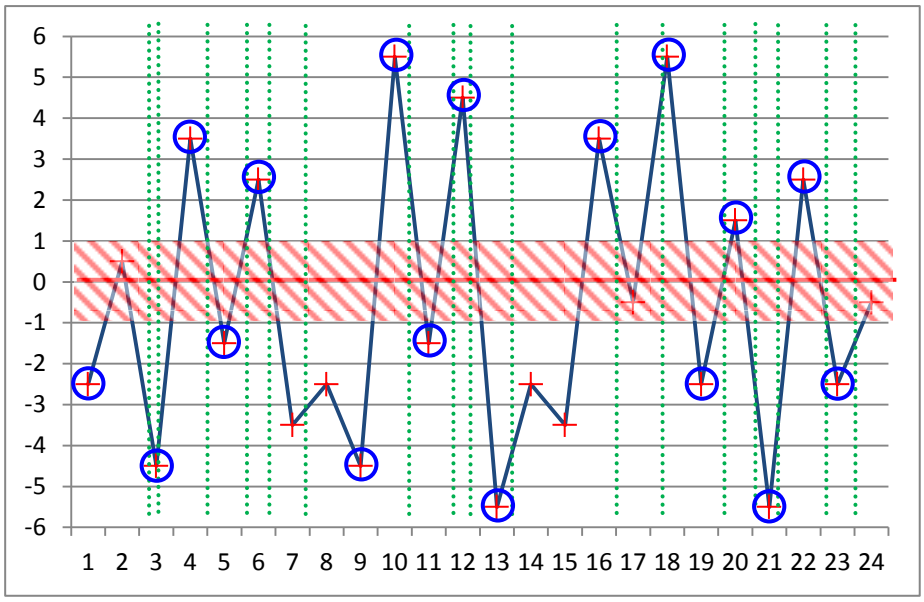

Figure 10: Values retained according to the PATRAM method

The values retained are circled in blue.

In numerical form, this is: -3,-5,4,-2,3,-5,6,-2,5,-6,4,6,-3,2,-6,3,-3.

RainFlow method

The RainFlow method counts the load cycles and thus provides information on the variations rather than the deceleration levels. This method is more complex and is the subject of the AFNOR standard A03-406. A simplified description is given below.

Let us consider the previous signal composed of 24 extrema hereafter called A_i. A variation is defined by $\Delta_i = A_{i+1} - A_i$.

Δ_i is considered as a cycle and applied in the counting procedure when $\Delta_i < \Delta_{i-1}$ and $\Delta_i < \Delta_{i+1}$ (1).

The cycles are extracted by covering the entire signal with the above-defined procedure (i varying from 2 to 23). The variations not meeting condition (1) form the residual variance. The residual variance is then duplicated before applying the counting procedure once again. All the load cycles are extracted in this manner.

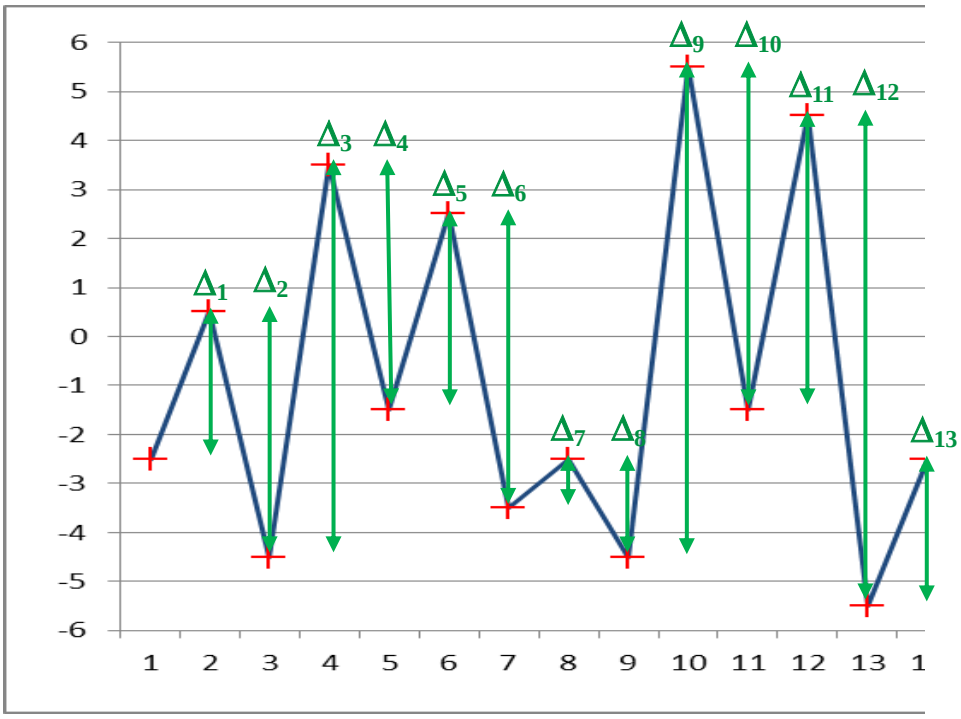

Figure 11: Values retained according to the RainFlow method

Based on the example above, Δ_2 is not considered as a cycle and is therefore not retained since $\Delta_2>\Delta_1$ does not meet condition (1). However, we checked that $\Delta_5<\Delta_4$ and $\Delta_5<\Delta_6$; Δ_5 was therefore retained (amplitude: 5 g).

We obtained the variations in the table below by applying the procedure to the entire signal:

Table 1: Counting the load cycles according to the RainFlow method

Range of cycle (g)	1	2	3	4	5	6	7	8	9	10	11
Number of cycles	2	0	0	3	2	1	0	1	0	0	2

The results obtained represent the amplitudes of the cycles, which is why the values do not have a sign (contrary to the PATRAM method).

Accelerograms

Noise

The recordings show background noise of about 0.3 g. As the transport package experienced low deceleration levels (about 1 g), filtering was required to eliminate this background noise so the signals could be used.

The recording was switched on 13 minutes before the truck's departure. This part of the recording was used to study the background noise alone.

Figure 12: Raw signals (channel 0 and 1, sensor 1, X and Y axes)

The following figure shows the Fourier transform (FT) for the two signals above:

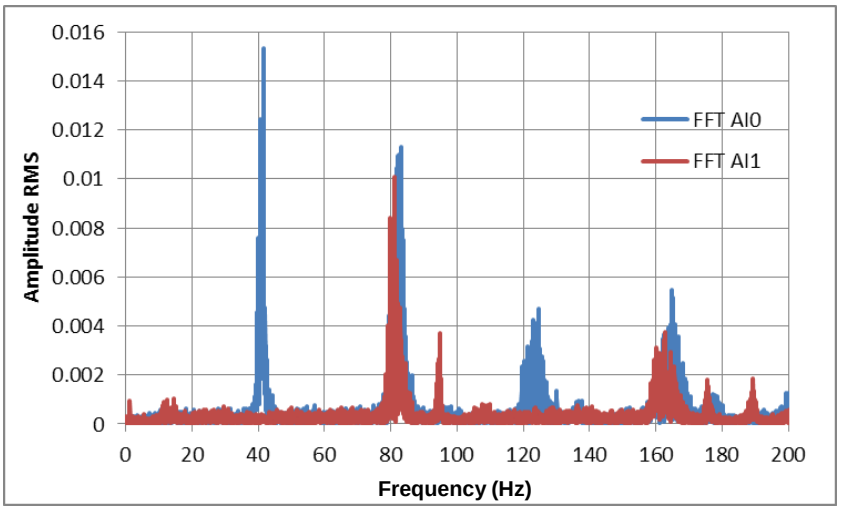

Figure 13: Fourier transform of the raw signals in Figure 12

Two fundamental components are visible at 40 Hz and 80 Hz for channels 0 and 1 respectively, as well as several harmonics.

To eliminate noise, the signals were filtered with a Butterworth low-pass filter from 4 to 20 Hz.

The following curves show the signal of sensor 1 along the x axis, both raw and filtered at 20 Hz:

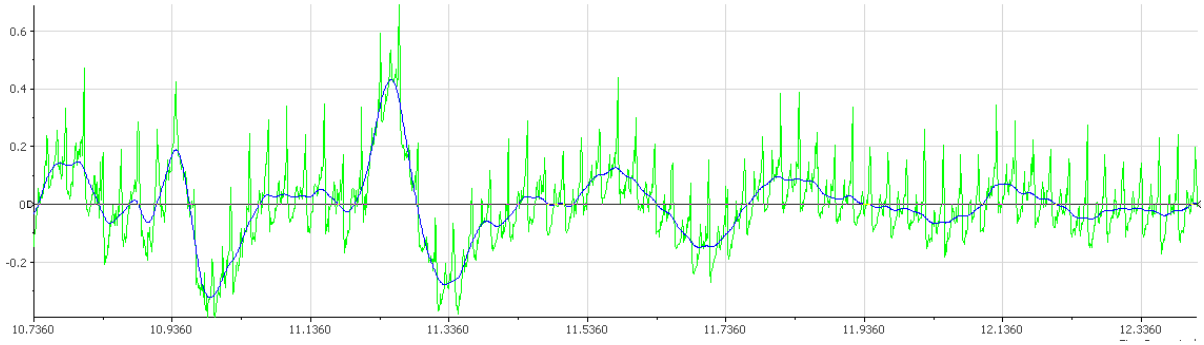

Figure 14: Acceleration curve both unfiltered and filtered at 20 Hz (acceleration in g, time in s)

The noise recorded by the accelerometers is analysed in greater detail below to determine its cause.

Analysis of the background noise recorded by the sensors

The signal generated by the accelerometers was studied using another data acquisition system at a much higher sampling frequency to the one used during the transport operation (1 million samples per second instead of 1000).

The following graph shows the parasitic signal that was recorded (the accelerometer was idle):

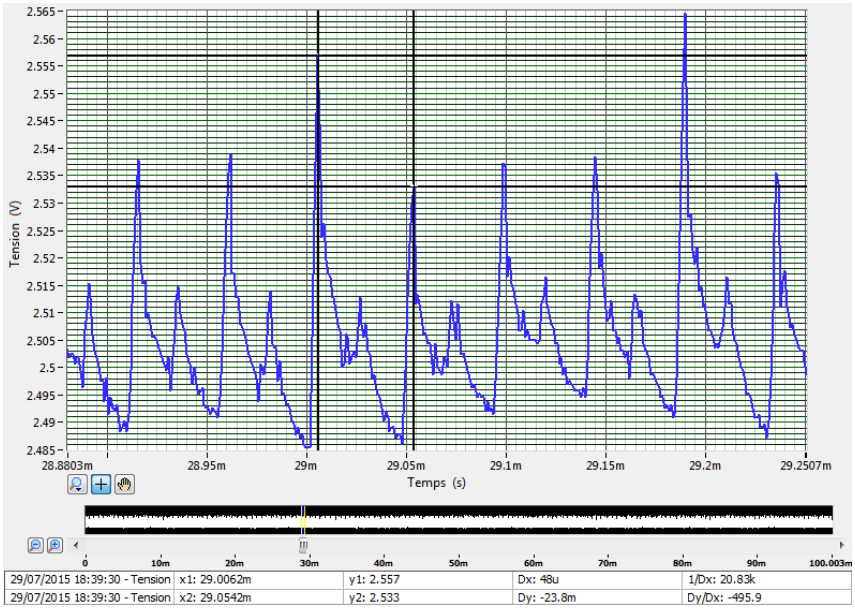

Figure 15: Parasitic signal recorded with the accelerometer idle

The recording shows a parasitic signal at high frequency (above the sampling frequency). This signal is the cause of an aliasing phenomenon (foldover distortion) which occurs during data acquisition on the road at a much lower frequency.

There are two possible solutions for eliminating (reducing) this aliasing phenomenon:

1- Collecting data at a frequency that is at least two times higher than the parasitic signal (40 kHz), before filtering the resulting signal at the required frequency (1 kHz) using an anti-aliasing filter. This is the most efficient solution but unfortunately it is not applicable due to the recording time and the size of the related file.

2- Filtering the signal before the recording machine (responsible for the aliasing phenomenon) by using an analogue filter. The filter's maximum frequency is half of the sampling frequency (500 Hz).

The following graph shows the recording of a signal that was taken in a car on the road. The first accelerometer was directly connected to the recorder. The second accelerometer is connected by adding a first-order low-pass filter with a cut-off frequency of 300 Hz between the accelerometer and the recorder:

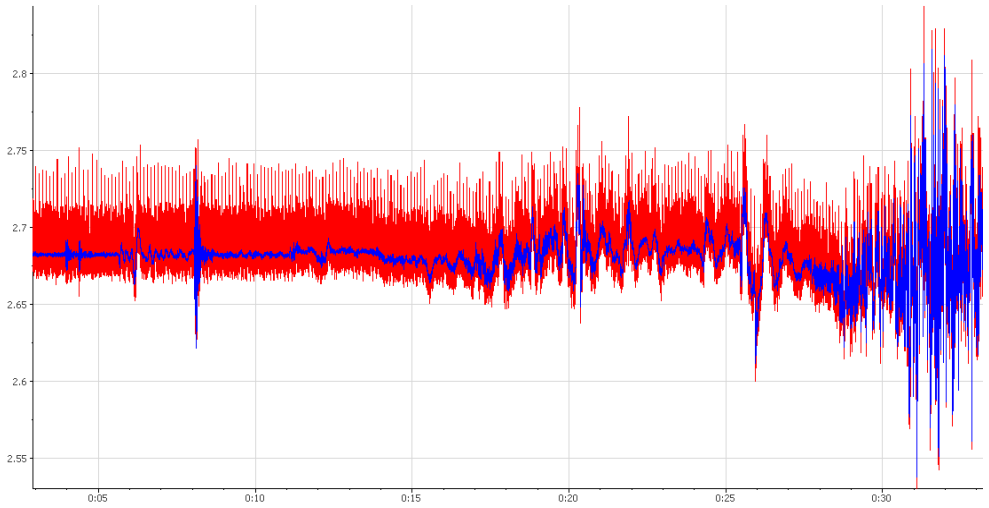

Figure 16: Signal recorded in a car on the road without a low-pass filter

Voltage in V (200 mV = 1 g)

In blue: sensor with filter In red: sensor without filter

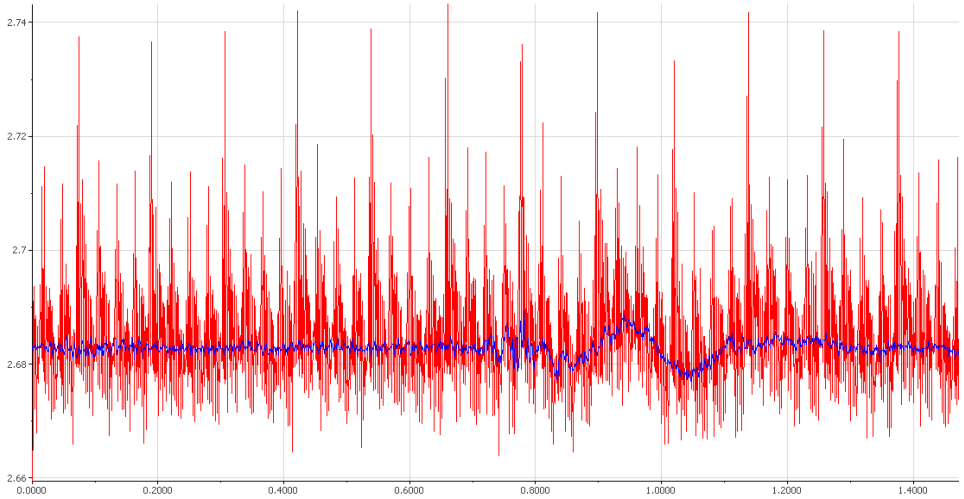

Figure 17: Signal recorded in a car on the road with a low-pass filter

Voltage in V (200 mV = 1 g)

In blue: sensor with filter In red: sensor without filter

The peak voltage of the signal recorded by the idle accelerometers was: 80 mV for the unfiltered accelerometer and 4 mV for the filtered accelerometer. As the sensor sensitivity was 200 mV, the background noise recorded by the unfiltered accelerometer represented about 0.4 g instead of 0.02 g for the filtered accelerometer.

The level of background noise with filtering at 300 Hz - 0.02 g is acceptable with respect to the size of the classes defined for post-processing: 0.2 g (ratio between the size of classes and the background noise is equal to 10).

Examples of recorded events

Transverse accelerograms (y axis) during a left bend at t = 19 min.

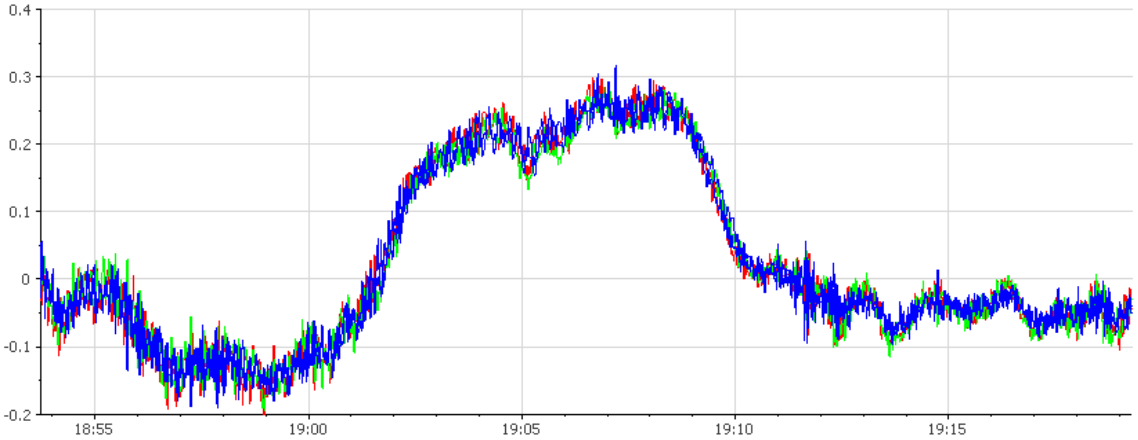

Figure 18: Transverse accelerations during a left bend (acceleration in g, time in s, y axis, superimposition of the 4 sensors)

Longitudinal acceleration (x axis) during "sudden" breaking at the 23-minute mark:

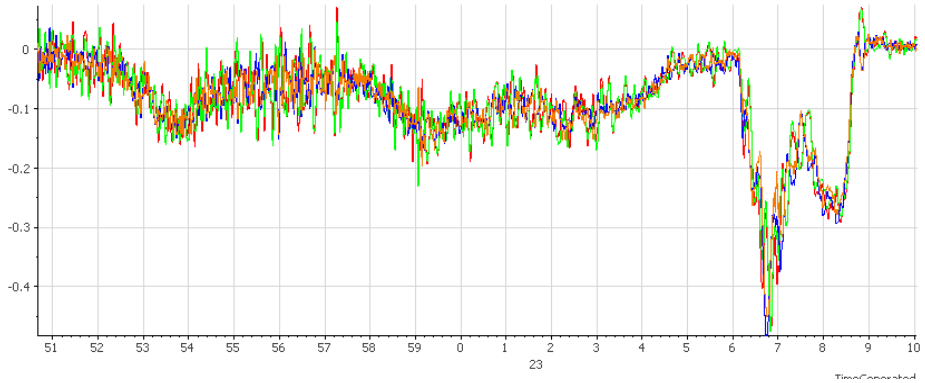

Figure 19: Longitudinal accelerations during sudden breaking (acceleration in g, time in s, x axis, superimposition of the 4 sensors)

Vertical resonance phenomenon on the motorway at the 55-minute mark:

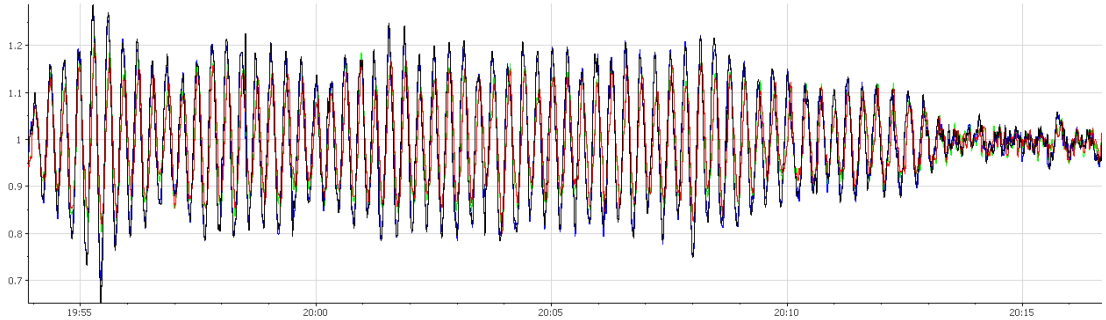

Figure 20: Vertical resonance (accelerometers 1 to 4, z axis)

The acceleration level was higher for the two rear accelerometers. The resonance frequency was 3.2 Hz.

Trip on the national road

The data provided in this section concern the distance covered on the national road: 18.2 km.

The acceleration peaks are ranked in the 0.1g classes. The class value indicated corresponds to the mean value of the acceleration range in question.

Counting using the PATRAM method

The signals were first filtered at 20 Hz to eliminate the background noise.

The vertical acceleration includes gravitational acceleration; it is therefore:

- equal to 1 when idle
- less than 1 during acceleration towards the ground
- greater than 1 during acceleration towards the sky.

The following tables show the acceleration peaks recorded for all the accelerometers.

Table 2: Number of acceleration peaks recorded for each accelerometer (PATRAM method)

Sensor 1/ top rear				
Accélération (g)	X	Y	Accélération (g)	Z
-0.95	0	0	0.05	0
-0.85	0	0	0.15	0
-0.75	0	0	0.25	0
-0.65	0	0	0.35	0
-0.55	0	0	0.45	0
-0.45	1	0	0.55	0
-0.35	0	9	0.65	1
-0.25	11	11	0.75	8
-0.15	137	170	0.85	285
-0.05	5183	3189	0.95	5247
0.05	5333	3525	1.05	5226
0.15	228	72	1.15	297
0.25	6	6	1.25	20
0.35	1	3	1.35	1
0.45	0	0	1.45	0
0.55	0	0	1.55	0
0.65	0	0	1.65	0
0.75	0	0	1.75	0
0.85	0	0	1.85	0
0.95	0	0	1.95	0

Sensor 2/ top front				
Accélération (g)	X	Y	Accélération (g)	Z
-0.95	0	0	0.05	0
-0.85	0	0	0.15	0
-0.75	0	0	0.25	0
-0.65	0	0	0.35	0
-0.55	0	0	0.45	0
-0.45	1	0	0.55	2
-0.35	0	11	0.65	4
-0.25	16	9	0.75	42
-0.15	126	162	0.85	483
-0.05	4991	3166	0.95	5984
0.05	5292	3115	1.05	6841
0.15	222	84	1.15	495
0.25	11	8	1.25	36
0.35	0	2	1.35	4
0.45	0	0	1.45	1
0.55	0	0	1.55	1
0.65	0	0	1.65	0
0.75	0	0	1.75	0
0.85	0	0	1.85	0
0.95	0	0	1.95	0

Sensor 3/ bottom rear				
Accélération (g)	X	Y	Accélération (g)	Z
-0.95	0	0	0.05	0
-0.85	0	0	0.15	0
-0.75	0	0	0.25	0
-0.65	0	0	0.35	0
-0.55	0	0	0.45	0
-0.45	1	1	0.55	0
-0.35	0	5	0.65	1
-0.25	5	11	0.75	5
-0.15	47	144	0.85	244
-0.05	4167	4184	0.95	6331
0.05	4780	4528	1.05	5373
0.15	50	64	1.15	253
0.25	0	7	1.25	11
0.35	0	3	1.35	1
0.45	0	0	1.45	0
0.55	0	0	1.55	0
0.65	0	0	1.65	0
0.75	0	0	1.75	0
0.85	0	0	1.85	0
0.95	0	0	1.95	0

Sensor 4/ bottom front				
Accélération (g)	X	Y	Accélération (g)	Z
-0.95	0	0	0.05	0
-0.85	0	0	0.15	0
-0.75	0	0	0.25	0
-0.65	0	0	0.35	0
-0.55	0	0	0.45	0
-0.45	1	0	0.55	2
-0.35	0	7	0.65	3
-0.25	6	10	0.75	40
-0.15	49	99	0.85	499
-0.05	5499	5311	0.95	5229
0.05	6760	4800	1.05	5358
0.15	56	47	1.15	493
0.25	0	7	1.25	38
0.35	0	1	1.35	5
0.45	0	0	1.45	1
0.55	0	0	1.55	1
0.65	0	0	1.65	0
0.75	0	0	1.75	0
0.85	0	0	1.85	0
0.95	0	0	1.95	0

The following two tables show the acceleration peaks recorded by the top accelerometers and the two bottom accelerometers extrapolated over a distance of 1000 km.

Table 3: Number of acceleration peaks recorded by the top and bottom accelerometers, extrapolated over a distance of 1000 km (PATRAM method)

Top maximum over 1000 km				
Accélération (g)	X	Y	Accélération (g)	Z
-0.95	0	0	0.05	0
-0.85	0	0	0.15	0
-0.75	0	0	0.25	0
-0.65	0	0	0.35	0
-0.55	0	0	0.45	0
-0.45	55	0	0.55	109
-0.35	0	601	0.65	219
-0.25	874	601	0.75	2295
-0.15	7486	9290	0.85	26393
-0.05	283224	174262	0.95	326995
0.05	291421	192623	1.05	373825
0.15	12459	4590	1.15	27049
0.25	601	437	1.25	1967
0.35	55	164	1.35	219
0.45	0	0	1.45	55
0.55	0	0	1.55	55
0.65	0	0	1.65	0
0.75	0	0	1.75	0
0.85	0	0	1.85	0
0.95	0	0	1.95	0

Bottom maximum over 1000 km				
Accélération (g)	X	Y	Accélération (g)	Z
-0.95	0	0	0.05	0
-0.85	0	0	0.15	0
-0.75	0	0	0.25	0
-0.65	0	0	0.35	0
-0.55	0	0	0.45	0
-0.45	55	55	0.55	109
-0.35	0	383	0.65	164
-0.25	328	601	0.75	2186
-0.15	2678	7869	0.85	27268
-0.05	300492	290219	0.95	345956
0.05	369399	262295	1.05	293607
0.15	3060	3497	1.15	26940
0.25	0	383	1.25	2077
0.35	0	164	1.35	273
0.45	0	0	1.45	55
0.55	0	0	1.55	55
0.65	0	0	1.65	0
0.75	0	0	1.75	0
0.85	0	0	1.85	0
0.95	0	0	1.95	0

The following histogram shows the number of acceleration peaks obtained at the top of the transport package in three directions for a distance of 1000 km (table illustrating the top maximum over 1000 km is given above).

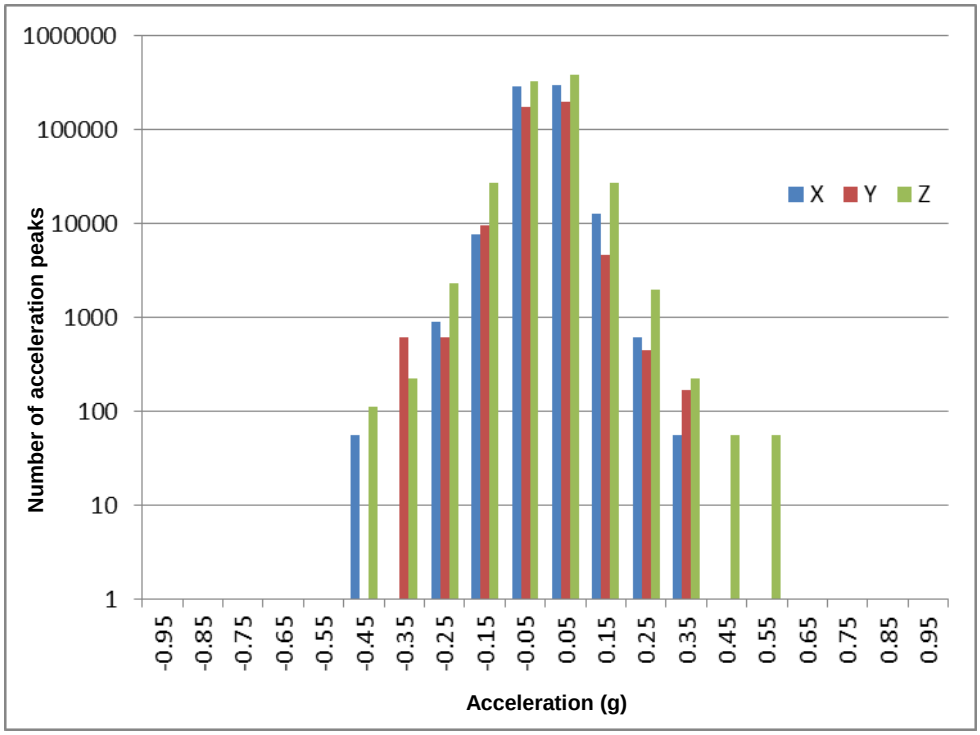

Figure 21: Distribution of acceleration peaks recorded at the top of the transport package (PATRAM method)

The gravitational acceleration was subtracted again; the scales are therefore identical for the x, y and z axes.

Counting with the RainFlow method

The signals were first filtered at 20 Hz.

The following tables show the acceleration peaks recorded for all the accelerometers.

Table 4: Number of acceleration peaks recorded with each accelerometer (RainFlow method)

Sensor 1/ top rear			
Accélération (g)	**X**	**Y**	**Z**
0.1	7622	7246	5525
0.2	248	224	174
0.3	65	27	198
0.4	5	8	15
0.5	3	4	5
0.6	0	4	2
0.7	1	2	0
0.8	0	0	0
0.9	0	0	0
1	0	0	0

Sensor 2/ top front			
Accélération (g)	**X**	**Y**	**Z**
0.1	8346	5578	10802
0.2	251	216	256
0.3	57	29	345
0.4	6	8	34
0.5	6	5	19
0.6	0	4	6
0.7	1	2	1
0.8	0	0	1
0.9	0	0	0
1	0	0	1

Sensor 3/ bottom rear			
Accélération (g)	X	Y	Z
0.1	7319	9351	8846
0.2	62	188	154
0.3	16	28	169
0.4	4	4	7
0.5	0	6	3
0.6	1	2	2
0.7	0	1	0
0.8	0	1	0
0.9	0	0	0
1	0	0	0

Sensor 4/ bottom front			
Accélération (g)	X	Y	Z
0.1	10464	8811	6117
0.2	73	124	265
0.3	15	23	349
0.4	5	3	33
0.5	0	5	20
0.6	1	3	5
0.7	0	1	0
0.8	0	0	2
0.9	0	0	0
1	0	0	1

The following two tables show the acceleration peaks recorded by the top accelerometers and the two bottom accelerometers extrapolated over a distance of 1000 km.

Table 5: Number of acceleration peaks recorded by the top and bottom accelerometers, extrapolated over a distance of 1000 km (RainFlow method)

Top maximum over 1000 km			
Accélération (g)	X	Y	Z
0.1	456066	395956	590273
0.2	13716	12240	13989
0.3	3552	1585	18852
0.4	328	437	1858
0.5	328	273	1038
0.6	0	219	328
0.7	55	109	55
0.8	0	0	55
0.9	0	0	0
1	0	0	55

Bottom maximum over 1000 km			
Accélération (g)	X	Y	Z
0.1	571803	510984	483388
0.2	3989	10273	14481
0.3	874	1530	19071
0.4	273	219	1803
0.5	0	328	1093
0.6	55	164	273
0.7	0	55	0
0.8	0	55	109
0.9	0	0	0
1	0	0	55

The following histogram shows the number of acceleration peaks obtained at the top of the transport package in three directions for a distance of 1000 km (table illustrating the top maximum over 1000 km is given above).

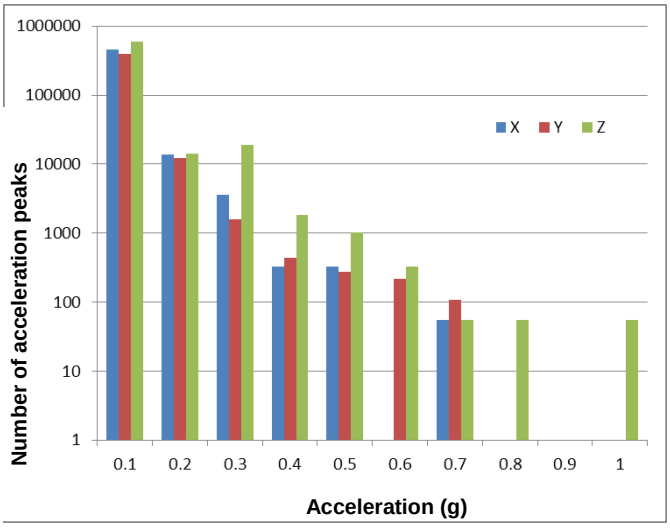

Figure 22: Distribution of acceleration peaks recorded at the top of the transport package (RainFlow method)

Trip on the motorway

The data provided in this section concern the distance covered on the motorway: 282 km.

The acceleration peaks have been ranked in the 0.1 g classes. The class value indicated corresponds to the mean value of the acceleration range in question.

Counting using the PATRAM method

The signals were first filtered at 20 Hz.

The following table shows the acceleration peaks recorded for all the accelerometers.

Table 6: Number of acceleration peaks recorded for each accelerometer (PATRAM method)

Sensor 1/ top rear				
Accélération (g)	X	Y	Accélération (g)	Z
-0.95	0	0	0.05	0
-0.85	0	0	0.15	0
-0.75	0	0	0.25	0
-0.65	0	0	0.35	0
-0.55	0	0	0.45	0
-0.45	0	0	0.55	0
-0.35	1	1	0.65	8
-0.25	42	10	0.75	101
-0.15	1015	205	0.85	2867
-0.05	74064	63182	0.95	59223
0.05	72990	67592	1.05	60584
0.15	836	292	1.15	3905
0.25	26	3	1.25	141
0.35	1	0	1.35	8
0.45	1	0	1.45	2
0.55	0	0	1.55	0
0.65	0	0	1.65	0
0.75	0	0	1.75	0
0.85	0	0	1.85	0
0.95	0	0	1.95	0

Sensor 2/ top front				
Accélération (g)	X	Y	Accélération (g)	Z
-0.95	0	0	0.05	0
-0.85	0	0	0.15	0
-0.75	0	0	0.25	0
-0.65	0	0	0.35	0
-0.55	0	0	0.45	2
-0.45	0	0	0.55	8
-0.35	0	2	0.65	50
-0.25	30	9	0.75	459
-0.15	1028	156	0.85	5340
-0.05	70664	51875	0.95	57351
0.05	69590	57840	1.05	58670
0.15	812	146	1.15	5464
0.25	18	3	1.25	485
0.35	3	0	1.35	52
0.45	0	0	1.45	16
0.55	0	0	1.55	2
0.65	0	0	1.65	1
0.75	0	0	1.75	2
0.85	0	0	1.85	0
0.95	0	0	1.95	0

Sensor 3/ bottom rear				
Accélération (g)	X	Y	Accélération (g)	Z
-0.95	0	0	0.05	0
-0.85	0	0	0.15	0
-0.75	0	0	0.25	0
-0.65	0	0	0.35	0
-0.55	0	0	0.45	0
-0.45	0	0	0.55	1
-0.35	0	1	0.65	7
-0.25	11	6	0.75	115
-0.15	126	169	0.85	4503
-0.05	65769	55034	0.95	67725
0.05	61117	62163	1.05	68422
0.15	60	158	1.15	8473
0.25	1	6	1.25	314
0.35	0	0	1.35	15
0.45	0	0	1.45	1
0.55	0	0	1.55	0
0.65	0	0	1.65	0
0.75	0	0	1.75	0
0.85	0	0	1.85	0
0.95	0	0	1.95	0

Sensor 4/ bottom front				
Accélération (g)	X	Y	Accélération (g)	Z
-0.95	0	0	0.05	0
-0.85	0	0	0.15	0
-0.75	0	0	0.25	0
-0.65	0	0	0.35	0
-0.55	0	0	0.45	3
-0.45	0	0	0.55	9
-0.35	0	1	0.65	59
-0.25	14	8	0.75	488
-0.15	278	132	0.85	5567
-0.05	73132	62038	0.95	53883
0.05	71976	67855	1.05	55440
0.15	666	158	1.15	5723
0.25	0	2	1.25	503
0.35	0	0	1.35	62
0.45	0	0	1.45	19
0.55	0	0	1.55	3
0.65	0	0	1.65	0
0.75	0	0	1.75	2
0.85	0	0	1.85	0
0.95	0	0	1.95	0

The following two tables show the acceleration peaks recorded by the top accelerometers and the two bottom accelerometers extrapolated over a distance of 1000 km.

Table 7: Number of acceleration peaks recorded by the top and bottom accelerometers, extrapolated over a distance of 1000 km (PATRAM method)

Top maximum over 1000 km				
Accélération (g)	X	Y	Accélération (g)	Z
-0.95	0	0	0.05	0
-0.85	0	0	0.15	0
-0.75	0	0	0.25	0
-0.65	0	0	0.35	0
-0.55	0	0	0.45	7
-0.45	0	0	0.55	28
-0.35	4	7	0.65	177
-0.25	149	35	0.75	1629
-0.15	3648	728	0.85	18951
-0.05	262840	224221	0.95	210172
0.05	259028	239872	1.05	215002
0.15	2967	1036	1.15	19391
0.25	92	11	1.25	1721
0.35	11	0	1.35	185
0.45	4	0	1.45	57
0.55	0	0	1.55	7
0.65	0	0	1.65	4
0.75	0	0	1.75	7
0.85	0	0	1.85	0
0.95	0	0	1.95	0

Bottom maximum over 1000 km				
Accélération (g)	X	Y	Accélération (g)	Z
-0.95	0	0	0.05	0
-0.85	0	0	0.15	0
-0.75	0	0	0.25	0
-0.65	0	0	0.35	0
-0.55	0	0	0.45	11
-0.45	0	0	0.55	32
-0.35	0	4	0.65	209
-0.25	50	28	0.75	1732
-0.15	987	600	0.85	19756
-0.05	259532	220162	0.95	240344
0.05	255430	240805	1.05	242817
0.15	2364	561	1.15	30069
0.25	4	21	1.25	1785
0.35	0	0	1.35	220
0.45	0	0	1.45	67
0.55	0	0	1.55	11
0.65	0	0	1.65	0
0.75	0	0	1.75	7
0.85	0	0	1.85	0
0.95	0	0	1.95	0

The following histogram shows the number of acceleration peaks obtained at the top of the transport package in three directions for a distance of 1000 km (table illustrating the top maximum over 1000km is given above).

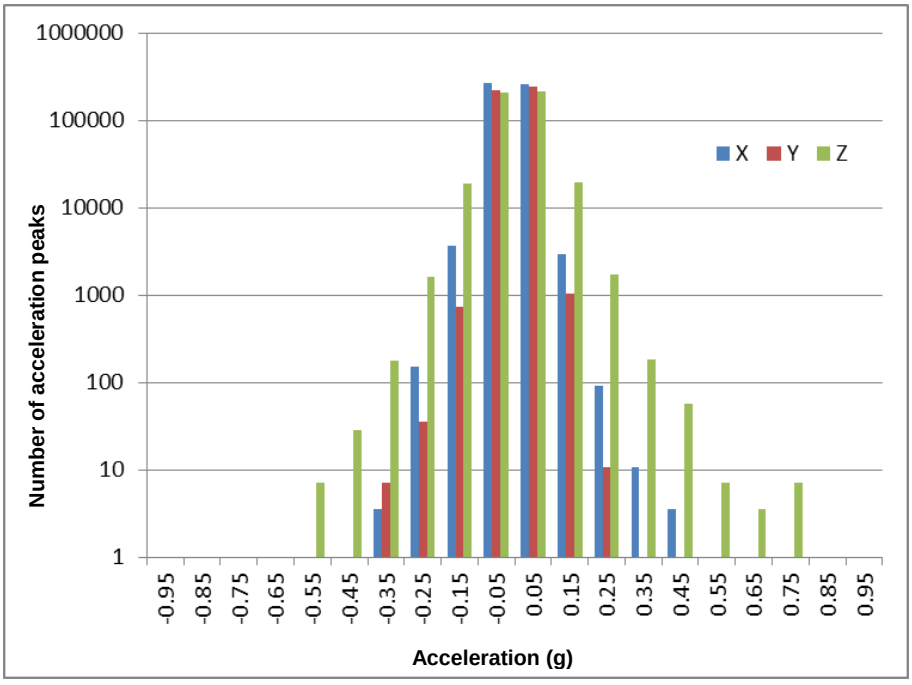

Figure 23: Distribution of acceleration peaks recorded at the top of the transport package (PATRAM method)

The gravitational acceleration was subtracted again; the scales are therefore identical for the x, y and z axes.

Counting with the RainFlow method

The signals were first filtered at 20 Hz.

The following tables show the acceleration peaks recorded for all the accelerometers.

Table 8: Number of acceleration peaks recorded for each accelerometer (RainFlow method)

Sensor 1/ top rear			
Accélération (g)	X	Y	Z
0.1	78177	72962	61381
0.2	1061	397	2191
0.3	391	56	2241
0.4	28	7	100
0.5	16	1	67
0.6	1	1	8
0.7	0	0	3
0.8	1	0	2
0.9	0	0	0
1	0	0	0
1.1	0	0	0
1.2	0	0	0
1.3	0	0	0

Sensor 2/ top front			
Accélération (g)	X	Y	Z
0.1	74330	62082	59429
0.2	1042	228	2451
0.3	396	42	4065
0.4	20	6	228
0.5	10	2	339
0.6	3	1	37
0.7	0	0	27
0.8	0	0	10
0.9	0	0	7
1	0	0	0
1.1	0	0	1
1.2	0	0	3
1.3	0	0	0

Sensor 3/ bottom rear			
Accélération (g)	X	Y	Z
0.1	72201	67619	70171
0.2	139	233	5506
0.3	22	55	3648
0.4	8	6	225
0.5	1	2	86
0.6	0	1	9
0.7	0	0	6
0.8	0	0	0
0.9	0	0	1
1	0	0	0
1.1	0	0	0
1.2	0	0	0
1.3	0	0	0

Sensor 4/ bottom front			
Accélération (g)	X	Y	Z
0.1	80466	73109	56014
0.2	793	205	2745
0.3	73	46	4135
0.4	12	6	275
0.5	0	1	336
0.6	0	1	44
0.7	0	0	32
0.8	0	0	16
0.9	0	0	3
1	0	0	4
1.1	0	0	0
1.2	0	0	0
1.3	0	0	2

The following two tables show the acceleration peaks recorded by the top accelerometers and the two bottom accelerometers extrapolated over a distance of 1000 km.

Table 9: Number of acceleration peaks recorded by the top and bottom accelerometers, extrapolated over a distance of 1000 km (RainFlow method)

Top maximum over 1000 km			
Accélération (g)	X	Y	Z
0.1	277436	258929	217830
0.2	3765	1409	8698
0.3	1405	199	14426
0.4	99	25	809
0.5	57	7	1203
0.6	11	4	131
0.7	0	0	96
0.8	4	0	35
0.9	0	0	25
1	0	0	0
1.1	0	0	4
1.2	0	0	11
1.3	0	0	0

Bottom maximum over 1000 km			
Accélération (g)	X	Y	Z
0.1	285559	259451	249024
0.2	2814	827	19540
0.3	259	195	14674
0.4	43	21	976
0.5	4	7	1192
0.6	0	4	156
0.7	0	0	114
0.8	0	0	57
0.9	0	0	11
1	0	0	14
1.1	0	0	0
1.2	0	0	0
1.3	0	0	7

The following histogram shows the number of acceleration peaks obtained at the top of the transport package in three directions for a distance of 1000 km (table illustrating the top maximum over 1000km is given above).

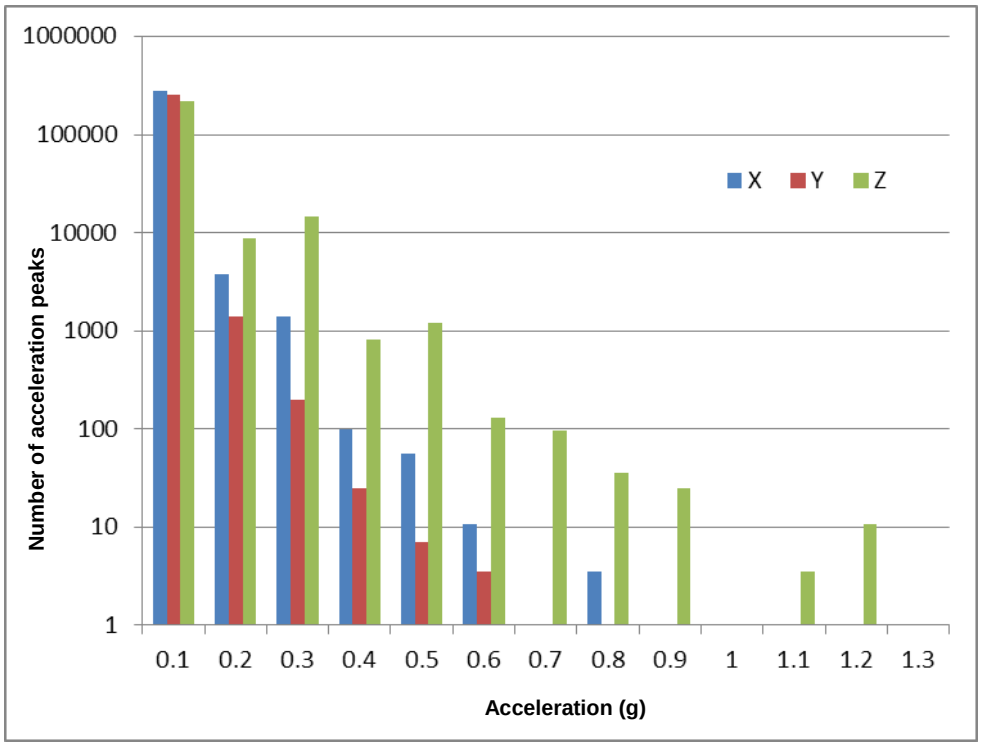

Figure 24: Distribution of acceleration peaks recorded at the top of the transport package (RainFlow method)

Results

Extrema

Table 10: Extrema measured from the signals filtered at 20 Hz

Accelerometer	Channel	Dir.	Min.	Max.	Absolute value
1	0	X	-0.32	0.43	0.43
	1	Y	-0.36	0.28	0.36
	2	Z	0.60	1.48	0.48
2	4	X	-0.30	0.37	0.37
	5	Y	-0.35	0.29	0.35
	6	Z	0.46	1.73	0.73
3	8	X	-0.25	0.21	0.25
	9	Y	-0.40	0.30	0.40
	10	Z	0.56	1.45	0.45
4	12	X	-0.28	0.19	0.28
	13	Y	-0.39	0.29	0.39
	14	Z	0.42	1.78	0.78
Max. at the top of the transport package	0 & 4	X	-0.32	0.43	0.43
	1 & 5	Y	-0.36	0.29	0.36
	2 & 6	Z	0.46	1.73	0.73
Max. on the trailer	8 & 12	X	-0.28	0.21	0.28
	9 & 13	Y	-0.40	0.30	0.40
	10 & 14	Z	0.42	1.78	0.78

The acceleration varies within -0.4 g and 0.4 g in the horizontal plane.
Vertically speaking, the acceleration varies between 0.4 g and 1.8 g (gravity ranges between these values).

Acceleration levels for the entire trip

The results given in this section concern the entire trip, i.e. national road and motorway. To make it easier to use these results, the number of acceleration peaks have been extrapolated over a distance of 1000 km. The number of peaks for each class has therefore been divided by the distance covered and multiplied by 1000.

PATRAM method

Table 11: Distribution of the acceleration peaks at the top of the transport package for a distance of 1000 km (PATRAM counting method)

Top maximum over 1000 km				
Accélération (g)	**X**	**Y**	**Accélération (g)**	**Z**
-0.95	0	0	**0.05**	0
-0.85	0	0	**0.15**	0
-0.75	0	0	**0.25**	0
-0.65	0	0	**0.35**	0
-0.55	0	0	**0.45**	7
-0.45	3	0	**0.55**	33
-0.35	3	43	**0.65**	180
-0.25	193	70	**0.75**	1670
-0.15	3883	1250	**0.85**	19408
-0.05	264128	221213	**0.95**	217333
0.05	261049	237031	**1.05**	224726
0.15	3546	1253	**1.15**	19861
0.25	123	37	**1.25**	1736
0.35	13	10	**1.35**	187
0.45	3	0	**1.45**	57
0.55	0	0	**1.55**	10
0.65	0	0	**1.65**	3
0.75	0	0	**1.75**	7
0.85	0	0	**1.85**	0
0.95	0	0	**1.95**	0

RainFlow method

Table 12: Distribution of the acceleration peaks at the top of the transport package for a distance of 1000 km (RainFlow counting method)

Top maximum over 1000 km			
Accélération (g)	**X**	**Y**	**Z**
0.1	288379	267331	240584
0.2	4373	2070	9022
0.3	1537	283	14698
0.4	113	50	873
0.5	73	23	1193
0.6	10	17	143
0.7	3	7	93
0.8	3	0	37
0.9	0	0	23
1	0	0	3
1.1	0	0	3
1.2	0	0	10
1.3	0	0	0

Comparison between the motorway and national road

The following table shows the ratio between the number of acceleration peaks obtained on the national road with that obtained on the motorway.

Table 13: Ratio between the number of acceleration peaks on the national road and the number of acceleration peaks on the motorway (RainFlow method)

Rainflow: Ratio national road / motorway			
Accélération (g)	**X**	**Y**	**Z**
0.1	1.6	1.5	2.7
0.2	3.7	8.7	1.6
0.3	2.5	8.0	1.3
0.4	3.3	17.6	2.3
0.5	5.8	38.6	0.9
0.6	0.0	61.8	2.5
0.7	oo	oo	0.6
0.8	0.0	0.0	1.5
0.9	0.0	0.0	0.0
1	0.0	0.0	oo
1.1	0.0	0.0	0.0
1.2	0.0	0.0	0.0
1.3	0.0	0.0	0.0

In any given category, there is a division by 0 when the number of acceleration peaks on the national road is not zero but the number of peaks on the motorway is zero, which is why we have used the symbol for infinity (oo) in the table.

This table reveals many more acceleration peaks on the national road than on the motorway, particularly on the y axis (transverse). This can be explained by the very few bends encountered on the motorway.

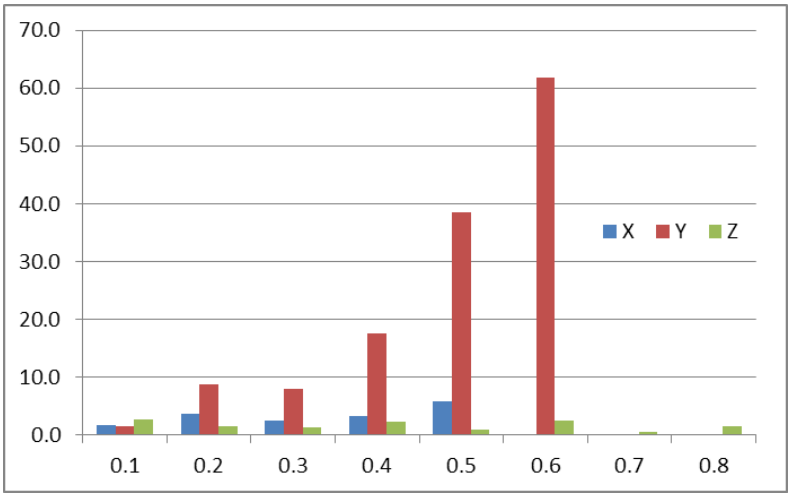

Table 25: Histogram of the ratio between the number of acceleration peaks on the national road and that on the motorway (RainFlow method)

Comparison of the RainFlow method with the PATRAM method

In a similar manner to the previous comparison, this distribution represents the ratio between the number of acceleration peaks counted with the RainFlow method and those counted with the PATRAM method.

Table 14: Ratio between the number of acceleration peaks counted with RainFlow and the number of acceleration peaks counted with PATRAM

Ratio Rainflow method / PATRAM method			
Accélération (g)	**X**	**Y**	**Z**
0.1	0.8	1.1	0.8
0.2	0.7	0.9	0.3
0.3	2.4	1.5	4.4
0.4	6.0	0.6	4.3
0.5	6.0	oo	6.3
0.6	0.0	oo	6.0
0.7	oo	oo	oo
0.8	0.0	0.0	oo
0.9	0.0	0.0	0.0
1	0.0	0.0	oo
1.1	0.0	0.0	0.0
1.2	0.0	0.0	0.0
1.3	0.0	0.0	0.0

The symbol oo indicates the fact that acceleration peaks were counted with RainFlow but not with PATRAM (division by 0).

The number of acceleration peaks is higher for the high acceleration values with the RainFlow method than with PATRAM.

The deceleration level reached is higher when the RainFlow method is used: 1 g compared with 0.6 g using PATRAM.

Comparison between the LR144 results obtained with PATRAM and the results given in the 1989 PATRAM article

The measurements recorded between La Hague and Tihange were presented at the PATRAM conference in 1989 [1] and have since been re-digitalised. The representativeness of the digitalised information is not perfect given the quality of the document and the use of logarithmic scales, but it nonetheless remains sufficient to compare this recording with the measurements taken during the LR144 transport.

The following two tables show the distribution resulting from the 1989 PATRAM tests on the one hand, and the distribution measured during the LR144 transport operation (extrapolated to a distance of 1000 km) on the other hand. To be comparable with reference [1], the acceleration classes for the distribution in Table 11 (acceleration levels for the full trip using the PATRAM method) were

modified as follows:

- The acceleration classes ranging between -0.2 g and 0.2 g were deleted.
- The size of the classes were modified and changed from 0.1 g and 0.2 g.

Table 15: Comparison of the acceleration peak distribution between the LR144 test and the 1989 PATRAM test (PATRAM method)

LR144 / Top maximum over 1000 km			
Accélération (g)	X	Y	Z
-2.1	0	0	0
-1.9	0	0	0
-1.7	0	0	0
-1.5	0	0	0
-1.3	0	0	0
-1.1	0	0	0
-0.9	0	0	0
-0.7	0	0	0
-0.5	3	0	40
-0.3	197	113	1850
0.3	137	47	1923
0.5	3	0	67
0.7	0	0	10
0.9	0	0	0
1.1	0	0	0
1.3	0	0	0
1.5	0	0	0
1.7	0	0	0
1.9	0	0	0
2.1	0	0	0

1989 PATRAM test over 1000 km			
Accélération (g)	X	Y	Z
-2.1	0	0	5
-1.9	0	0	5
-1.7	3	2	13
-1.5	5	25	13
-1.3	19	31	25
-1.1	94	188	50
-0.9	313	438	250
-0.7	625	1250	1875
-0.5	1875	3750	18750
-0.3	4375	56250	250000
0.3	7500	18750	250000
0.5	3125	2500	25000
0.7	1875	1250	3750
0.9	625	313	500
1.1	188	125	125
1.3	56	31	50
1.5	19	13	31
1.7	5	3	19
1.9	0	0	13
2.1	0	0	6

The number of acceleration peaks recorded above 0.2 g is lower for the LR144 trip by several orders of magnitude. Little information is available on the data acquisition system used during the 1989 PATRAM tests, and whether the signals were filtered or not. The number of acceleration peaks recorded at low (but not insignificant) levels seems rather surprising in [1]. Between -0.3 g and 0.3 g on the z axis, for instance, we counted 500,000 peaks over 1000 km, i.e. 1 peak every 2 m on average.

One of the possible explanations is related to the transport configuration. During the 1989 PATRAM road test, the NTL 8/3 package was transported horizontally and anchored by its spindles. It was therefore most probably a "rigid" anchoring set-up than the LR144 configuration that was responsible for high-frequency vibrations and at higher acceleration levels.

Raw results without filtering

The following two tables show the number of acceleration peaks obtained with the PATRAM counting method on an unfiltered signal.

Table 16: Comparison of the acceleration peak distribution according to the PATRAM method between the top of the transport package (left) and the trailer (right)

LR144 / Top maximum over 1000 km			
Accélération (g)	X	Y	Z
-2.5	0	0	0
-2.3	0	0	0
-2.1	0	0	0
-1.9	0	0	0
-1.7	0	0	0
-1.5	0	0	0
-1.3	0	0	0
-1.1	0	0	0
-0.9	0	0	0
-0.7	6	4	32
-0.5	1360	1949	5162
-0.3	1455606	2337334	2620169
0.3	1831648	2446366	2700260
0.5	222352	122163	192871
0.7	21	19	354
0.9	0	0	14
1.1	0	0	2
1.3	0	0	0
1.5	0	0	0
1.7	0	0	0
1.9	0	0	0
2.1	0	0	0
2.3	0	0	0
2.5	0	0	0

LR144 / Bottom maximum over 1000 km			
Accélération (g)	X	Y	Z
-2.5	0	2	4
-2.3	0	2	9
-2.1	1	2	15
-1.9	5	14	9
-1.7	5	27	43
-1.5	16	67	123
-1.3	57	222	302
-1.1	177	665	688
-0.9	570	1956	1631
-0.7	2927	6765	5185
-0.5	21246	41988	35989
-0.3	2402309	2504021	2090531
0.3	2425206	2636816	2200900
0.5	129925	231209	181589
0.7	4205	7621	5247
0.9	993	2034	1278
1.1	274	797	450
1.3	79	310	162
1.5	21	105	61
1.7	6	32	33
1.9	2	7	15
2.1	0	3	4
2.3	0	5	5
2.5	0	4	4

It must be pointed out that the number of acceleration peaks is distorted by the background noise recorded on the sensors (particularly at low acceleration levels).

The two tables reveal the effect of filtering provided by the more flexible anchoring set-up and the mass of the LR144 package. The high acceleration peaks (above 0.7 g) at high frequency recorded on the trailer are not recorded at the top of the transport package.

Conclusion

The CEA and its subcontractor DEMA conducted acceleration measurements on the LR144 transport packing during a road trip without its radioactive contents under routine transport conditions.

The objective of this measurement campaign was to determine the acceleration peaks and the number of acceleration cycles in three directions so as to use these values in fatigue design calculations for the anchor parts.

The accelerations were measured continuously on the transport package and the trailer during a trip between the CEA Marcoule Centre in the south of France and Mâcon.

The measurements were processed according to both the type of road taken (motorway or national road) and the counting algorithm applied to the signal (RainFlow or PATRAM). Filtering was required to eliminate background noise so the signals could be used.

The following results were obtained:

- Accelerations vary between -0.4 g and 0.4 g in the horizontal plane.

- Accelerations vary between 0.4 g and 1.8 g (gravity falls between these values) in the vertical plane (z).

The results were then compared by extrapolating them to cover a distance of 1000 km:

- Depending on the type of road: more acceleration peaks are recorded on the national road than on the motorway, in particular along the y axis (transverse), which is due to the small number of bends on the motorway.

- Depending on the signal processing method: the number of acceleration peaks is higher for the high acceleration values when RainFlow is used compared with PATRAM. The deceleration level reached is also higher when the RainFlow method is used.

- Depending on the accelerometer location: the high acceleration peaks at high frequency recorded on the trailer are not recorded at the top of the transport package. These results reveal the effect of filtering provided by the more flexible anchoring set-up and the mass of the LR144 package.

- Depending on the transport package tested: the acceleration peaks recoded and their number are much lower for the LR144 transport package compared with the NTL 8/3 package presented during the 1989 PATRAM conference. These differences can be explained by the different signal filtering process and by the anchor system used for the NTL 8/3 package which was probably more rigid than the LR144 frame. The measurement results presented at the 1989 PATRAM conference remain conservative with respect to the fatigue design of the package anchor devices.

References

[1] “Measurement of the acceleration undergone by the trunnions of irradiated fuel transport flasks during normal use”, D. Pujet (Nuclear Transport Limited, Paris) and P. Malesys (Transnucléaire, Paris), PATRAM 1989, June 11-16, 1989, Washington DC, USA.